

CEAS Interlibrary Loan Request to Photocopy

Univ. of Cincinnati Langsam Library Interlibrary Loan [libill@ucmail.uc.edu]

Sent: Thursday, July 23, 2015 10:20 AM

To: CEAS Library (engrlib2)

Cc: Library ILL (libill)

This request has been forwarded from University of Cincinnati Langsam Library ILL.
Request Information for ILLiad Transaction Number: 388124

Transaction Date: 7/23/2015 10:18:49 AM

Call Number: TP156.M3 I58 v.7-8(2005-06)

Location: CEAS Journals LIB USE ONLY

Journal Title : International journal of transport phenomena.

Journal Vol: 8

Journal Issue: 2

Journal Month:

Journal Year: 2006

Article Title: Transient Heat Transfer Analysis on a Heat Pipe With Experimental Validation

Article Author: G Gutierrez, J Catano, T Jen, Q Liao

Article Pages: 165-179

Borrower: UMC

ILL Number: 151483252

Lending String: MHY,*CIN

Patron:

Shipping Address:

University of Maryland, McKeldin Library, Interlibrary Loan,
College Park, MD 20742-7011,

Ariel:

Odyssey: docdel.umd.edu

Fax: 301-314-2487

E-Mail Address: docdel@umd.edu

NOTICE: This material may be protected by COPYRIGHT LAW (Title 17 U.S. Code).

Transient Heat Transfer Analysis on a Heat Pipe with Experimental Validation

GUATAVO GUTIERREZ¹, JUAN CATAÑO¹, TIEN-CHIEN JEN^{2*} AND QUAN LIAO²

¹ *Mechanical Engineering Department University of Puerto Rico
Mayaguez, PR 00681-9045*

² *Mechanical Engineering Department University of Wisconsin, Milwaukee
Milwaukee, WI 53211*

In this study, a transient analysis of the performance of a heat pipe with a wick structure is performed. A complete formulation of the equation governing the operation of a heat pipe during transient conditions are presented and discussed. For the vapor flow, the conventional Navier-Stokes equations are used. For the liquid flow in the wick structure, which is modeled as a porous media, volume averaged Navier-Stokes equations are adopted. The energy equation is solved for the solid wall and wick structure of the heat pipe. The energy and momentum equations are coupled through the heat flux at the liquid-vapor interface that defines the suction and blowing velocities for the liquid and vapor flow. The evolution of the vapor-liquid interface temperature is coupled through the heat flux at this interface that defines the mass flux to the vapor and the new saturation conditions to maintain a fully saturated vapor at all time. A control volume approach is used in the development of the numerical scheme. A parametric study is conducted to study the effect of different parameters that affect the thermal performance of the heat pipe. And experimental setup is developed and numerical results are validated with experimental data. The results of this study will be useful for the heat pipe design and implementation in processes that are essentially transient.

Keywords: Transient heat transfer, heat pipe, numerical analysis

1. INTRODUCTION

Heat pipe applications can be found in many areas of engineering and technology, like aerospace, heat exchanger, electronic cooling, solar technology and cooling of the tip of a drill [13] just to mention a few. Heat pipes offer an effective alternative to removing

heat without significant increases in operating temperatures. A heat pipe is a passive device that transports energy with relatively low temperature difference without the need of an external power supply. The components of a heat pipe are a sealed container (pipe wall and end caps), a wick structure, and a small amount of working fluid in equilibrium

*Corresponding Author: Email: jent@uwm.edu

with its own vapor. Typically, a heat pipe can be divided into three sections: evaporator section, adiabatic (transport) section and condenser section. The external heat load on the evaporator section causes the working fluid to vaporize. The resulting vapor pressure drives the vapor through the adiabatic section to the condenser section, where the vapor is condensed, releasing its latent heat of vaporization to the low temperature environment. The condensed working fluid is then pumped back by capillary pressure generated by the meniscus in the wick structure. Transport of heat can be continuous as long as there is enough capillary pressure generated to drive the condensed liquid back to the evaporator.

There is an extensive literature dedicated to heat pipes research. A detailed literature review on the state-of-art development in heat pipes can be found in Faghri [5] and Peterson [16]. Tournier and El-Genk [18] present a transient heat transfer model by numerically solving the Navier-Stokes equation and energy equation in the wick region and the energy equation in the solid wall. A coupling of the thermal with the hydrodynamic boundary condition through an energy balance at the interface was introduced. Subsequently, El-Genk and Huang [4] carried out an experimental investigation to validate the numerical solution. Harley and Faghri [11] present a transient lumped model and Cao and Faghri [2] developed a two-dimensional transient continuum model similar to the one presented by Tournier and El-Genk. Sobhan *et al.* [17] solves a conjugate problem for the vapor, wick structure and solid wall for a flat heat pipe with water as the working fluid, using volume-averaged Navier-Stokes equations in the porous media. All these models suffer from the disadvantages that either oversimplify the models or become very intense numerical simulation. Some other researchers [6],[19] concentrate on the startup of the heat pipe from a frozen condition, which are typical cases in high temperature heat pipe application using liquid metals as working fluids. In this study, the full formulation is presented and discussed but a simplified model is developed for the transient response of the heat pipe retaining

most of its main physical characteristics by solving the energy equation in the solid wall and wick region and updating the interface temperature by assuming a fully saturated condition in the vapor core. If the permeability of the pipe is very small, the flow in the wick can be assume stagnant without significance effect in the temperature response. The full conjugate problem has been solved by the author [10] and a full sensitivity analysis was performed to analyze the effect of different parameters in the operation of a heat pipe.

2. PHYSICAL MODEL AND MATHEMATICAL FORMULATION

The basic geometric parameters of the heat pipe and the coordinate system are shown in Figure 1. Geometric dimensions and input values are summarized in the Table 1. In this study, the working fluid used is water.

Heat fluxes at the evaporator and convection conditions at the condenser are considered uniform around the circumferential direction. Based on this assumption, the problem becomes axis-symmetric and all the derivatives with respect to the circumferential direction are zero. Thus, the problem becomes two-dimensional in cylindrical coordinates. The vapor and liquid flow are assumed laminar and incompressible. For the vapor flow in the core region of the heat pipe the conventional Navier-Stokes equations are applied. For the liquid flow in the wick structure, the conceptual model is a porous medium. In porous media, the Navier-Stokes equations are still valid but only for each fluid element inside the micro channel. However, due to the complex geometric configuration, the flow becomes very complicated and some kind of averaging is necessary to make the problem tractable mathematically. This idea is in some way similar to the time-averaging approach in turbulent flow. In porous media instead, a volume averaged of the Navier-Stokes equations is performed [1]. This volume-averaging to the Navier-Stokes equations yields:

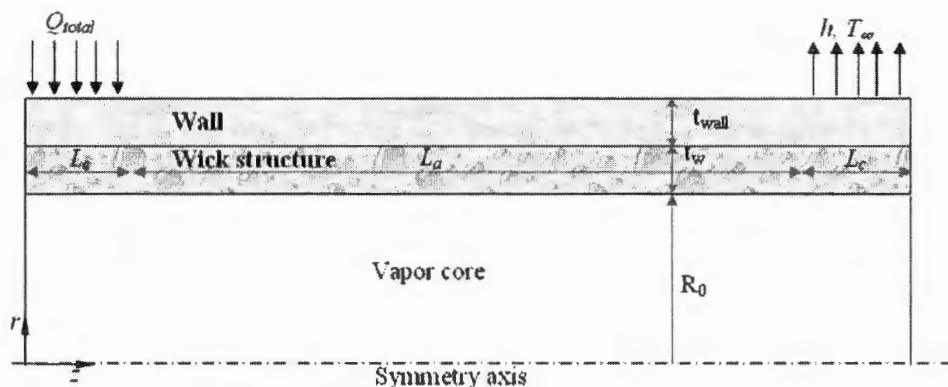


FIGURE 1
Physical domain and coordinate system.

TABLE I
Geometric dimensions and input values of the heat pipe.

Le	0.025 m	R₀	0.005 m
La	0.15 m	t_w	0.001 m
Lc	0.025 m	t_{wall}	0.001 m
k_s	401 W/m-°C	Cp_s	385 J/kg-°C

$$\frac{\partial(\rho \bar{v}_i)}{\partial t} + \frac{\partial(\rho \bar{v}_i \bar{v}_i)}{\partial x_j} = -\frac{\partial \hat{p}}{\partial x_i} + \frac{\partial}{\partial x_j} \left(\mu \frac{\partial \bar{v}_i}{\partial x_j} \right) - \rho \frac{\partial \bar{v}_i'^2}{\partial x_j} \delta_{ij} \quad (1)$$

Where \hat{p} is the reduced pressure, $\hat{p} = p - \rho gh$, h is the height of the heat pipe with respect to the horizontal position v_i and is a local spatial deviation in the "i" direction within the void space. The average velocity \bar{v}_i is related to the Darcy velocity \bar{V}_i by the Dupuit-Forchheimer relationship, $\bar{V}_i = \epsilon \bar{v}_i$, where ϵ is the porosity. Writing equation (1) in terms of the Darcy velocity yields:

$$\frac{1}{\epsilon} \frac{\partial(\rho \bar{V}_i)}{\partial t} + \frac{1}{\epsilon^2} \frac{\partial(\rho \bar{V}_i \bar{V}_i)}{\partial x_j} =$$

$$-\frac{\partial \hat{p}}{\partial x_i} + \frac{1}{\epsilon} \frac{\partial}{\partial x_j} \left(\mu \frac{\partial \bar{V}_i}{\partial x_j} \right) - \rho \frac{\partial \bar{V}_i'^2}{\partial x_j} \delta_{ij} \quad (2)$$

The term $\rho \frac{\partial \bar{V}_i'^2}{\partial x_j} \delta_{ij}$ represents viscous resisting force due to the variation of the flow in the micro-channels of the porous medium. At this point we have to introduce the porous medium model equivalent in

some way to the constitutive equations in the continuum model. We will assume that this resistance force is proportional to the average velocity at that point plus an additional term proportional to the square of the velocity and they are acting in a direction opposite to the local velocity:

$$-\rho \frac{\partial \bar{v}_i^2}{\partial x_j} \delta_{ij} = -\frac{\mu}{K} \bar{v}_i - \frac{C_F}{\sqrt{K}} \rho |\bar{v}_i| \bar{v}_i \quad (3)$$

Where K is called the "permeability" of the porous medium and the coefficient C_F is the Ergun's constant which value is approximately 0.55. The first term on the right hand side is called the Darcy term and the second one is called the Forchheimer term, which is due to the dispersion effect in the porous media. Note that the Forchheimer term is usually small when the Darcy velocity is small. Introducing this model into Equation (2):

$$\begin{aligned} \frac{1}{\varepsilon} \frac{\partial (\rho \bar{v}_i)}{\partial t} + \frac{1}{\varepsilon^2} \frac{\partial (\rho \bar{v}_i \bar{v}_j)}{\partial x_j} = -\frac{\partial \bar{p}}{\partial x_i} + \frac{1}{\varepsilon} \frac{\partial}{\partial x_j} \\ \left(\mu \frac{\partial \bar{v}_i}{\partial x_j} \right) - \frac{\mu}{K} \bar{v}_i - \frac{C_F}{K^{0.5}} \rho |\bar{v}_i| \bar{v}_i \end{aligned} \quad (4)$$

Defining a "reduced velocity" $V_i = \frac{\bar{v}_i}{\varepsilon}$ and substituting into Equation (4):

$$\begin{aligned} \frac{\partial (\rho V_i)}{\partial t} + \frac{\partial (\rho V_i V_j)}{\partial x_j} = \\ -\frac{\partial \bar{p}}{\partial x_i} + \frac{\partial}{\partial x_j} \left(\mu \frac{\partial V_i}{\partial x_j} \right) - \varepsilon \frac{\mu}{K} V_i - \varepsilon^2 \frac{C_F}{K^{0.5}} \rho |V_i| V_i \end{aligned} \quad (5)$$

Defining a "pore Reynolds number" as:

$$Re_p = \rho_l \frac{\bar{v}_i \sqrt{K}}{\mu_l} \quad (6)$$

Writing the last term of the right hand side of equation (4), the Forchheimer term, in term of the pore Reynolds number and comparing with the Darcy term yields:

$$-\frac{\mu}{K} \bar{v}_i - \frac{C_F}{K^{0.5}} \rho |\bar{v}_i| \bar{v}_i = -\frac{\mu}{K} \bar{v}_i (1 + C_F Re_p) \quad (7)$$

If $(C_F Re_p)$ is of order one, the Forchheimer term is of the same order as the Darcy term. It can be seen that Equation (5) reduces to the equation of the vapor core of the heat pipe by letting $\varepsilon = 1$ and K equals to infinity. This provides a convenient formulation for the numerical solution.

In cylindrical coordinates and with axis-symmetric conditions implied, the mass and momentum equations can be written as:

Conservation of mass

$$\frac{1}{r} \frac{\partial}{\partial r} (r V_r) + \frac{\partial V_z}{\partial z} = 0 \quad (8)$$

Momentum equation in the radial direction

$$\begin{aligned} \frac{\partial (\rho V_r)}{\partial t} + \frac{1}{r} \frac{\partial (\rho r V_r V_r)}{\partial r} + \frac{\partial (\rho V_r V_z)}{\partial z} = -\frac{\partial \bar{p}}{\partial r} \\ + \mu \left(\frac{1}{r} \frac{\partial}{\partial r} (r \frac{\partial V_r}{\partial r}) + \frac{\partial^2 V_r}{\partial z^2} - \frac{V_r}{r^2} \right) - \varepsilon \frac{\mu}{K} V_r - \varepsilon^2 \frac{C_F}{\sqrt{K}} \rho V_r |V_r| \end{aligned} \quad (9)$$

Momentum equation in the axial direction

$$\begin{aligned} \frac{\partial (\rho V_z)}{\partial t} + \frac{1}{r} \frac{\partial (\rho r V_z V_r)}{\partial r} + \frac{\partial (\rho V_z V_z)}{\partial z} = -\frac{\partial \bar{p}}{\partial z} \\ + \mu \left(\frac{1}{r} \frac{\partial}{\partial r} (r \frac{\partial V_z}{\partial r}) + \frac{\partial^2 V_z}{\partial z^2} \right) - \varepsilon \frac{\mu}{K} V_z - \varepsilon^2 \frac{C_F}{\sqrt{K}} \rho V_z |V_z| \end{aligned} \quad (10)$$

Here V_r and V_z are the "reduced" radial and axial velocities respectively. Note that for the vapor, the reduced velocities are the actual velocities. For the liquid, the actual (Darcy) velocities are the reduced velocities times the porosity, $\bar{v}_i = V_i \varepsilon$. It is worth noting that using this formulation, the same formulation can be used to solve the flow in a two-dimensional flat heat pipe by just letting $r = 1$ and replace the coordinate r as the y coordinate perpendicular to the axial direction z .

The energy equation has the following form:

$$\frac{(\rho C_p)_m}{C_p} \frac{\partial T}{\partial t} + \frac{1}{r} \frac{\partial(\rho r V_r T)}{\partial r} + \frac{\partial(\rho V_z T)}{\partial z} = \frac{\mu}{Pr} \left(\frac{1}{r} \frac{\partial}{\partial r} \left(r \frac{\partial T}{\partial r} \right) + \frac{\partial^2 T}{\partial z^2} \right) \quad (11)$$

Here, Pr is the Prandtl number written as $Pr = \frac{\mu C_p}{k}$

where k is the thermal conductivity. For the wick structure, the thermal conductivity is computed as an effective conductivity k_m of the non-heterogeneous medium that can be modeled as [3]:

$$k_m = k_s \left(\frac{2 + k_l/k_s - 2\varepsilon(1 - k_l/k_s)}{2 + k_l/k_s + \varepsilon(1 - k_l/k_s)} \right) \quad (12)$$

The subscript "s" accounts for the properties of the solid material of the wick and subscript "l" for the properties of the working fluid. C_p is the specific heat of the liquid for the wick domain and the specific heat of the solid for the wall domain. The effective heat capacity $(\rho C_p)_m$ that appears in the transient term is computed as [3]:

$$(\rho C_p)_m = (1 - \varepsilon)(\rho C_p)_s + \varepsilon(\rho C_p)_l \quad (13)$$

For solid walls k_m is just the conductivity of the solid wall k_s and $(\rho C_p)_m$ is the heat capacity of the solid wall; the velocity field in the solid wall is zero and the energy equation therefore reduces to the heat conduction equation.

3. BOUNDARY CONDITIONS AND INITIAL CONDITION

At the end caps of the heat pipe ($z=0$ and $z=L$), the radial and axial velocities are zero (impermeable wall and no-slip condition). The impermeable condition at the end cap near the tip can be justified by the fact that no evaporation or condensation is taking place at this end caps due to the lack of a wick structure there (i.e., no liquid is accumulated there). At the exterior boundary of the wick structure ($R=R_0+t_w$), the radial and axial velocities are zero too (impermeable wall and no-slip condition). A symmetry condition is applied in the symmetric axis of the vapor core.

Evaporation and condensation at the interface of the vapor and wick of the heat pipe are modeled as blowing and suction velocities [5], which are related to the local heat transfer rate as:

$$\bar{V}_w = \pm \frac{q(z)}{2\pi R_0 \rho h_{fg}} \quad \text{and} \quad V_w = \pm \frac{\bar{V}_w}{\varepsilon} \quad (14)$$

Where $q(z)$ is the local rate of heat transfer per unit length, ρ is the density of the vapor when calculating the input and output velocity of the vapor core and switches to the density of the liquid for the input and output of the wick structure; h_{fg} is the latent heat of vaporization. The positive sign corresponds to a suction action in the condenser for the liquid and a blowing action for the vapor; the negative sign corresponds to a blowing action in the evaporator for the vapor and a suction action for the liquid. The local heat transfer rate $q(z)$ is calculated from the solution of the energy equation and this is the way that the momentum and energy equations are coupled. It is further assumed that a uniform heat flux prevails at the evaporator section and is applied at the surface of the heat pipe ($R=R_0+t_w+t_{wall}$, see Fig. 1). To be able to proceed with the transient calculation, an assumption is needed for the thermal boundary condition at the outer surface of the heat pipe in the condensation section. A convection boundary condition is prescribed, assuming a constant heat transfer coefficient and a reference temperature T_∞ is imposed, which is equal to the ambient temperature. The outer surface between the evaporation and condensation sections is assumed insulated. The temperature at the liquid-vapor interface is calculated as part of the solution assuming that the vapor is always completely saturated. The saturation temperature is related to the saturation pressure of the vapor through the Clausius-Clayperon equation and this interface temperature must be updated at each time step. Here, instead of the Clausius-Clayperon equation, saturation conditions were curve fitted using an exponential regression for water steam values. In this way, density at the vapor core is related to saturation temperature. Then, the interface temperature is updated at each time step following the saturation line. The density at the current time step $n+1$ is updated as:

$$\rho_{n+1} = \rho_n + \frac{\dot{m} \Delta t}{\mathcal{V}} \quad (15)$$

Where $\dot{m} = \int_0^L \rho_n V_{\text{int}} dx$ is the mass flux per unit width, Δt is the time step and \mathcal{V} is the volume of the vapor core. V_{int} is the flow velocity at the interface. The initial condition is set equal to the ambient temperature T_∞ , everywhere at $t=0$.

4. NUMERICAL MODELING

For numerical purposes, it is useful to have a generic conservation equation, from which the equations of conservation of mass, momentum and energy are obtained. This universal conservation equation in cylindrical coordinates can be written as:

$$\frac{\partial(\rho\phi)}{\partial t} + \frac{1}{r} \frac{\partial(\rho r V_r \phi)}{\partial r} + \frac{\partial(\rho V_z \phi)}{\partial z} = \Gamma \left(\frac{1}{r} \frac{\partial}{\partial r} \left(r \frac{\partial \phi}{\partial r} \right) + \frac{\partial^2 \phi}{\partial z^2} \right) + S_\phi \quad (16)$$

Where ϕ is a generic property, which is defined as the intensive property of the system (e.g., for continuity, mass has to be conserved, so $\phi=1$), Γ is

the diffusivity for the generic property ϕ , S_ϕ is the source term. For the energy equation the transient term has the form showed in Equation (11). It can be seen from Table 2 that the governing equations can be reproduced from this generic equation. The main advantage of the generic conservation equation is that only one equation of the same form is required in the numerical program developing. Note that the pressure gradient is included in the source term just for convenience in the notation. In actual computation, however, this term is treated separately since the pressure field has to be calculated as part of the solution. A pressure correction (or pressure equation) is derived from the momentum equation to enforce mass conservation. This is the basis of the SIMPLE-like algorithms [15].

The term $\mu \frac{V_r}{r^2}$ that appears in cylindrical

coordinates in Equation (9) is treated implicitly as part of the central coefficient. For the liquid flow, the contribution of the porous media model is moved to the left hand side of the equations and treated implicitly as part of the central coefficient.

No boundary condition was prescribed at the interface between the solid wall and the wick

TABLE 2
Terms in the generic conservation equation.

ϕ	Γ	S_ϕ	Equation
1	-	0	continuity
V_r	μ	$-\frac{\partial \hat{p}}{\partial r}$	r-momentum
V_z	μ	$-\frac{\partial \hat{p}}{\partial z}$	z-momentum
T	$\frac{k_m}{C_p}$	0	energy equation

structure. However a unique heat flux must prevail at this interface. Numerically, the solid domain and the porous domain can be solved separately and iterates until matching the heat flux at the interface. Another more efficient way is to solve both domains together as a conjugate problem. Prescribing a large number for the viscosity in the solid domain will guarantee a zero velocity field for the solid domain and the interface temperature is calculated as part of the solution [15].

A variable grid is used to have a better resolution near the interface. In the axial direction the grid is generated in three zones of 16 control volumes in the evaporator and condenser zones and 50 control volumes in the adiabatic zone. In the radial direction the grid is generated in two zones of 10 control volumes in the wick region and 10 control volumes in the solid wall zone. The variable grid is created using an expansion coefficient, which is chosen close to unity to maintain a globally second order accuracy in space. A grid independent test confirmed that this grid was good enough and was used for all the calculations. A control volume approach is used to discretize the governing equations. The diffusion terms in the generic equation are discretized using a centered difference scheme. For the convection terms a power law scheme [15] is used. The pressure velocity coupling is solved using the SIMPLEC algorithm [21]. For details of the discretization see Ferziger and Peric [8].

5. NUMERICAL PROCEDURE

1. Solve the temperature field for the wall and wick regions using the current values of the velocity and temperature fields. A Dirichlet (constant surface temperature) boundary condition is applied at the vapor-liquid interface.
2. Calculate the vapor-liquid interface velocities based on the heat transfer rate obtained in step 1 using Equation (17). The heat transfer rate is computed from the temperature field in the wick structure using the Fourier's law. The heat transfer can be neglected in the vapor core due to the low

conductivity of the vapor and practically uniform temperature field in the vapor domain [10].

3. Solve the momentum equations in the r and z directions simultaneously using the current values for pressure and velocities (in the first iteration a zero velocity and pressure field is assumed, except at the boundaries where the boundary conditions are applied). The liquid and vapor domains are solved sequentially.
4. Since the velocities obtained in Step 3 may not satisfy the continuity equation locally, the pressure correction equation is solved to obtain the necessary corrections for the velocity field. Note that using the SIMPLEC algorithm the pressure does not need a correction.
5. Correct the velocity field until continuity is achieved.
6. Since the momentum equations may not be satisfied with the corrected velocities, repeat steps 3 to 6 until the residual of the momentum equations and pressure equation are less than a pre-assigned convergence criterion. Numerical grid convergence is needed to guarantee that the results are independent of the grid size and from the convergence value assigned for the residual of the linear system.
7. After convergences of momentum and continuity equations for the current time step, repeat steps 1 to 6 for the next time step and so on, updating the saturation temperature at the vapor-liquid interface using equation 18. Proceed to the next time step until a steady state condition is obtained.

6. RESULTS AND DISCUSSION

From the solution of the vapor flow, what is important for the thermal performance is how much the pressure drops in the vapor core. However, this pressure drop is very small, typically in the order of 10 to 20 Pa, thus the temperature in the vapor core can be assumed to be constant. From a numerical point of view, the more involved computation is the solution of the vapor but its velocity profiles does not play significant role in thermal performance of the heat

pipe, Gutierrez (2002). Under certain special conditions, for example, for longer heat pipes of liquid metal, which may result in high velocities in the vapor, the solution of the vapor could be important. However, for the dimensions of the heat pipe analyzed here, the vapor behaves very much isothermal. Regarding the solution of the liquid flow

in the wick structure, the kind of flow in the wick is pretty much governed by the hydraulic conductivity of the porous medium. For a sintered wick structure, this value is very small, in the order of 10^{-10} m and the flow is a Darcy flow. For the order of heat input tested in this paper, 10 W to 20 W, the velocities in the wick are very small, in the order of 1 mm/s and the

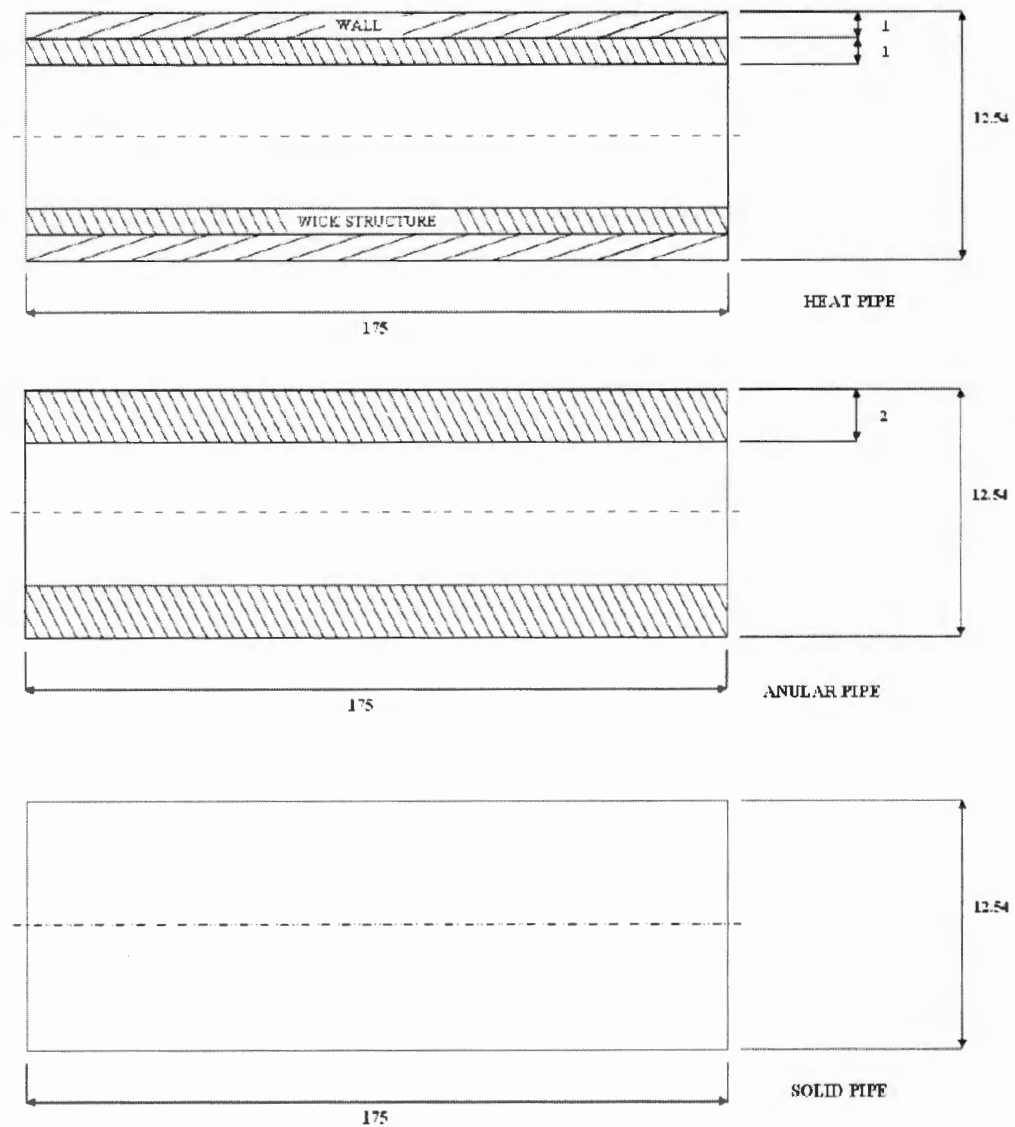


FIGURE 2
Pipe sizes in millimeters.

convection contribution of the flow is very small. With this consideration, it is possible to uncouple the hydrodynamic problem and thus significantly reducing the numerical effort. The only coupling that still is needed is the blowing and suction velocity calculated from Equation (14) to update the density with Equation (15) and calculate the current saturation temperature during the transient calculations. A comprehensive parametric study was carried out by comparing a heat pipe with a solid pipe and an annular pipe of pure copper of the same dimensions. This will give a better understanding of under what conditions the heat pipe operate more effectively compare with a pipe of pure conduction. The annular pipe was included to appreciate how a heat pipe will respond after dry out conditions. The results from the parametric study will subsequently be validated experimental data. A schematic of the heat pipe, solid pipe, and annual pipe with dimensions is given in Figure 2.

Figure 3 shows a comparison between a heat pipe, a solid pipe and an annular solid pipe of pure conduction for a heat input of 7 W and a heat transfer coefficient $h_c = 50 \text{ W/m}^2\text{K}$. The heat pipe has the following dimensions, 14 mm diameter and 175 mm long with outer wall thickness of 1 mm and the wick layer thickness of 1 mm. The lengths of the evaporation, adiabatic, and condensation sections are, 25 mm, 125 mm, and 25 mm, respectively. The solid pipe has the same dimension of the heat pipe, which is made of copper. The annular pipe is 2 mm thick and has the same dimension of the heat pipe, which is similarly made of copper and insulated in the internal wall. It can be seen from the figure that that the annular pipe is the fastest to respond since its thermal energy storage capacity is the lowest. Its temperature at the center of the evaporator rises to approximately 184°C at steady state condition. It takes about 3000 seconds to reach steady state temperature. On the contrary, the solid pipe responds much more slowly due to its larger mass and thermal energy storage capacity and even after 5000 seconds, it still has not reached a steady state condition. Its temperature in the evaporation zone is still rising (over 160°C) and approaching to a higher asymptotic temperature

(approximately 170°C). The heat pipe responds faster than the solid pipe and its temperature difference between evaporation and condensation is very small (all three curves for heat pipe are overlapped with one another). It requires almost the same time (3000 seconds) to reach the steady state temperature as for the annual pipe. However, under steady state conditions the heat pipe provides the lowest temperature in the evaporation zone.

Figure 4 shows the temperature response for the same conditions as Figure 2 but for a larger heat transfer coefficient $h_c = 500 \text{ W/m}^2\text{K}$. It can be seen that in this case the heat pipe is the fastest to respond and reaches steady state conditions (approximately 150 seconds) and clearly the lowest temperature (38°C) in the evaporator. For the annual pipe, it requires more than 400 seconds to reach steady state, and the temperature at evaporator region is over 70°C , which is approximately two times the temperature of the heat pipe. Similarly, the solid pipe is the slowest one to reach the steady state temperature; in evaporation region, its temperature rises above 50°C after 800 seconds, and still does not reach the steady state temperature. It can be seen that the heat pipe has a much stronger heat transfer capability than the other two types of pipe. It is worth noting that in all cases the temperature at the condensation approach to the same value. This temperature is controlled only by the heat input, the area of the condensation and the heat transfer coefficient through the Newton's law of cooling. Since these parameters are the same for all the cases, the condensation temperature should approach to the same value under steady state conditions.

Figure 5 shows the temperature responses for the same conditions as in Figure 3 and Figure 4, but in this case, the heat transfer coefficient, h_c , is $1,000 \text{ W/m}^2\text{K}$. In this case, the heat pipe reaches steady state in less than 100 seconds, with the lowest evaporation temperature at 32°C , compared to 300 seconds for steady state and 66°C in the evaporation zone for annual pipe. Again, the solid pipe has not reached steady state over more than 800 seconds and the maximum evaporation temperature may well above 50°C . It can be concluded that the higher the heat transfer coefficient the more effective of a heat pipe is with respect to a solid and annular tube of pure conduction.

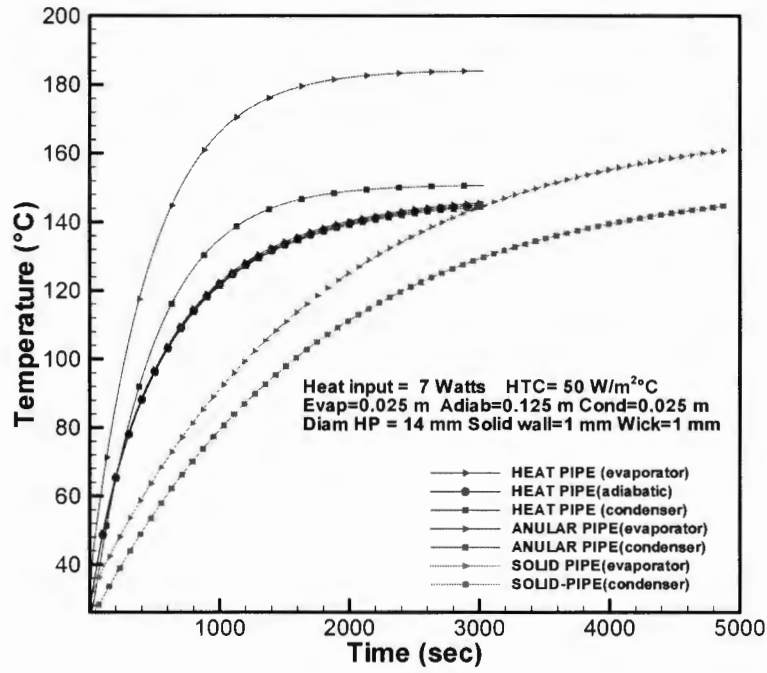


FIGURE 3
Comparison between a heat pipe, a solid and an annular pipe for $hc=50 \text{ W/m}^2 \text{ K}$.

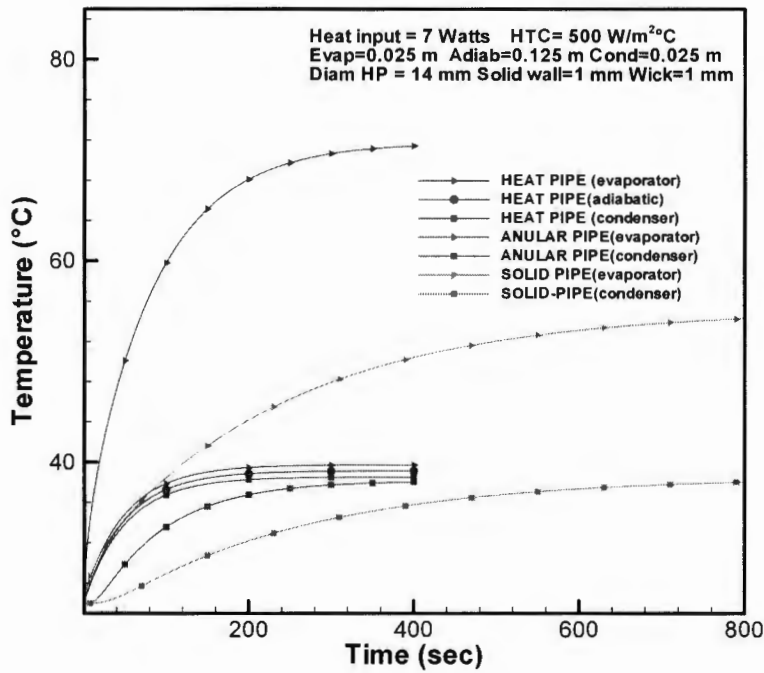


FIGURE 4
Comparison between a heat pipe, a solid and an annular pipe for $hc=500 \text{ W/m}^2 \text{ K}$.

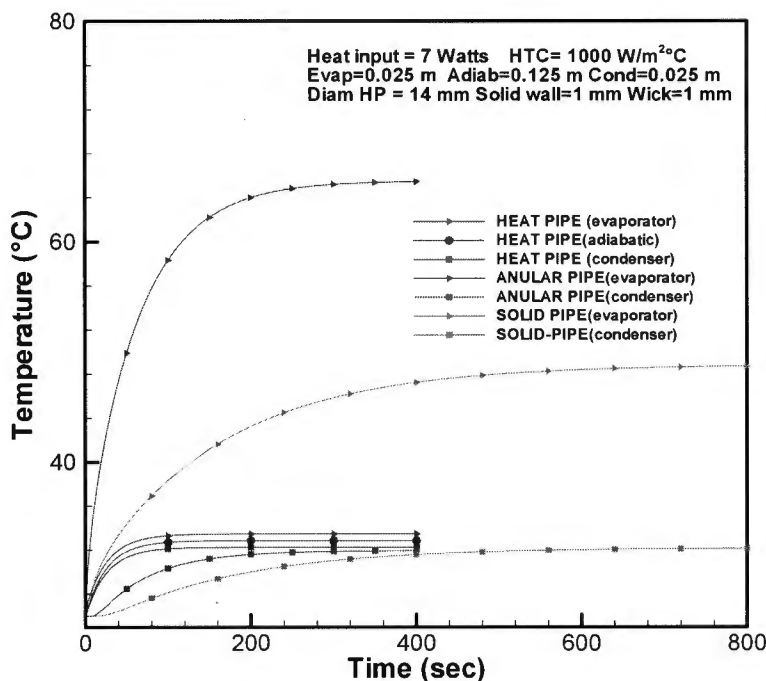


FIGURE 5
Comparison between a heat pipe and a solid and annular pipe for $hc=1000 \text{ W/m}^2 \text{ K}$.

Figure 6 shows a comparison among a heat pipe, a solid and an annular pipe of pure conduction for two different lengths. The two different lengths investigated here are, 17.5 cm and 25 cm. A heat transfer coefficient of $h_c = 2,000 \text{ W/m}^2 \text{ K}$ and a heat input of 20 W are used in this study. From this figure, it can be seen that the length of the heat pipe essentially has no effect on the temperature response in all three regions, evaporator region, adiabatic region and condenser region. However, it has a strong impact on the solid pipe and on the annular pipe. This is because the heat needs to conduct much longer distance before it can be removed from the convection at the evaporator end. A brief calculation shows that the Biot number for the solid and annual pipe is increased approximately by a factor of two, which means that the conductive resistance is two times as large as the shorter length ones. This again reveals that heat pipes can transport heat efficiently to a long distance (as long

as the capillary limit is not exceeded) without increasing the temperature in the evaporator zone. However, it cannot be concluded the same for the solid pipe and the annular pipe of pure conduction.

7. EXPERIMENTAL VALIDATION

The uncertainty of the experiment data is $\pm 2.5\%$, at the most, for steady state values, this is due mainly to uncertainty of the thermocouples (type T), the data acquisition system and the power supply system are also taken into account but only have a small contribution on the final uncertainty value; numerous experiments were performed and good repeatability is obtained, which agrees with the experimental uncertainty.

Figure 7 depicts a schematic diagram of the experimental setup. An electrical band heater is used as a heat input and a water-cooling jacket as a heat

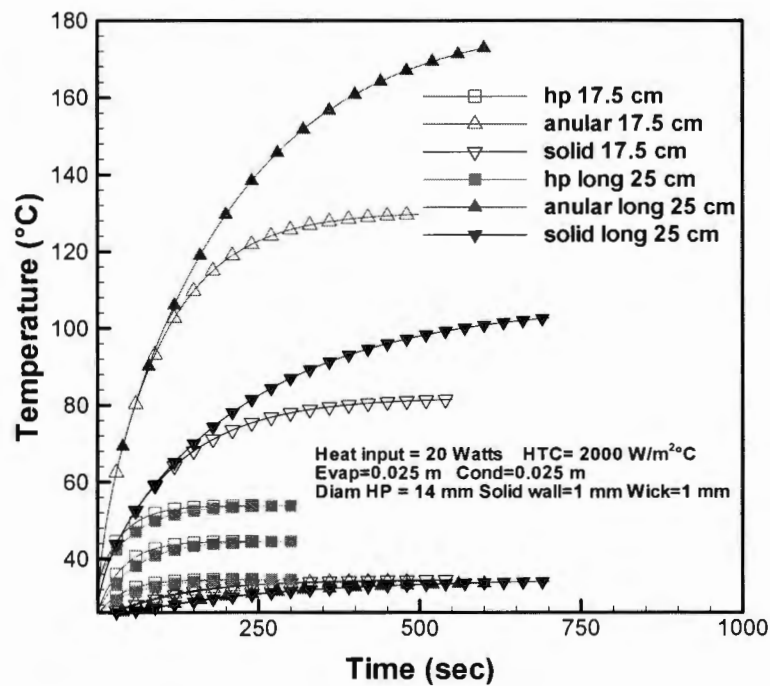


FIGURE 6
Effect on temperature response for the lengths of the heat pipe, solid and annual pipe.

sink in the condenser section of the heat pipe. The power input is controlled with a variable output transformer (variac) and the input current and voltage are recorded by the data acquisition system; the temperatures of the water are measured at the entrance and exit of the cooling jacket. The inlet temperature is maintained at a constant temperature, and the water flow rate is measured with a flow meter at the entrance of the cooling jacket. The band heater is coupled with the heat pipe using an aluminum block and the cooling jacket uses a liquid-tight cord grip to prevent leakage at the heat pipe-cooling jacket joint as shown in the figure. The system is insulated to prevent heat losses in the adiabatic section. Temperature measurements are made with T-type thermocouples placed in the middle of the evaporator, adiabatic and condenser sections on the heat pipe surface. The experimental

setup enables to test the heat pipe in any orientation and in real time data collections.

To compare experimental data with numerical simulation, the program is modified to incorporate the coupling aluminum block in the evaporator section. To keep the axis-symmetry, a third zone was added to the numerical model with the properties of the aluminum in the evaporator zone and a very low Prandtl number (10^{-20}) for the rest of the zone. This will guarantee a constant temperature there equal to T_{∞} in this zone.

The convection boundary condition is applied at the interior nodes of the external solid wall of the heat pipe in the condenser section; the convection coefficient is measured from the experimental data using the Newton law of cooling with an average of the temperature of the water at the entrance and exit of the cooling jacket as the bulk temperature of the

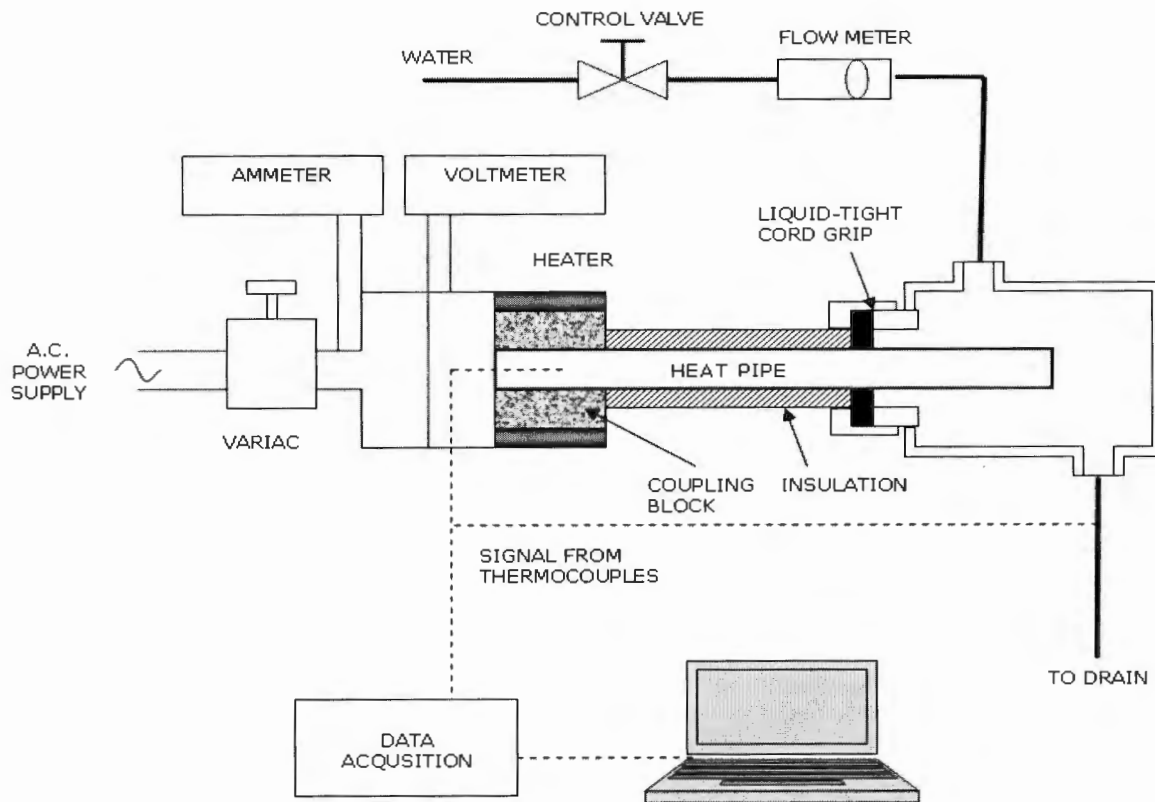


FIGURE 7
Schematic diagram of the experimental setup.

fluid and the temperature of the condenser section as the surface temperature. The heat transfer coefficient estimated by the water cooling jacket is approximately $h_c=410 \text{ W/m}^2\text{K}$.

The effective thermal conductivity, k_m , can also be calculated from the experimental data by the temperature difference between the evaporator and adiabatic zone temperatures after the heat pipe reaches the steady state condition, and this method is proved to be more accurate than the one obtained from Equation (12).

Figure 8 shows a comparison of experimental data and numerical results for a heat input of $Q=10.0 \text{ W}$. Temperatures are measured with T-type thermocouples at the middle of the evaporator, at

the middle of the adiabatic zone and at the middle of the condenser. The coupling block was an annular aluminum block 5.5 mm thick. It can be seen from the figure that the agreement in temperature at these three zones is reasonably good with some discrepancies during the initial transient region. This is probably due to contact resistance between the block and the heat pipe. However, the time required for the transient period is in very good agreement. This may be concluded that the fully saturation condition of the vapor at all times is a reasonable assumption. The experiments were also run in a vertical position and for the several level of heat inputs, no dry out condition was observed for the heat pipe.

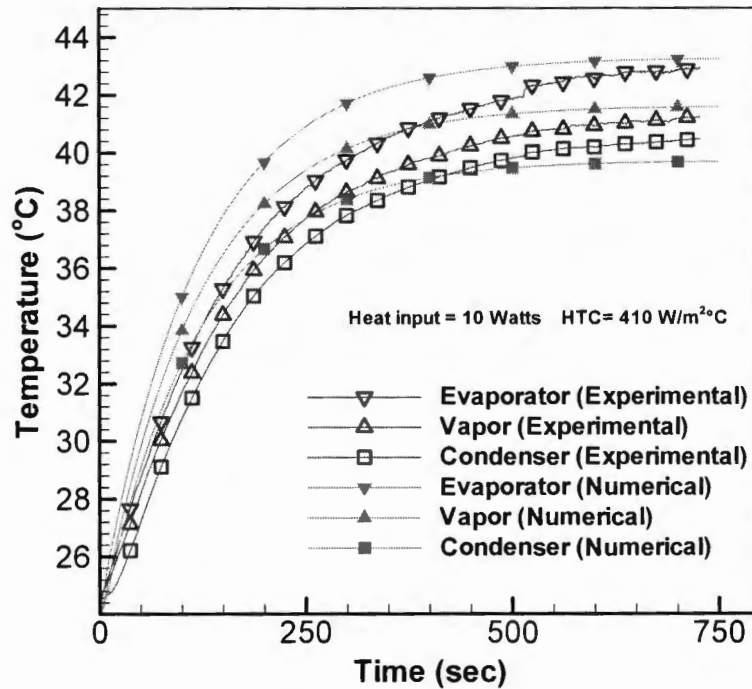


FIGURE 8
Comparison between experimental and numerical data for a heat input of 10W and $hc=410\text{W/m}^2\text{K}$.

ACKNOWLEDGEMENT

Dr. Gustavo Gutierrez appreciates the support to this of University of Puerto Rico-Mayaguez. Dr. Tien-Chien Jen would like to thank the National Science Foundation under GOALI program DMII 9908324, and UW System Applied Research for their financial support of the project.

NOMENCLATURE

C_F Ergun's constant, 0.55
 C_p specific heat [J/kg-°C]
 $(\rho C_p)_m$ effective heat capacity [J/m³-°C]
 h_c heat transfer coefficient at the condenser [W/m²-°C]
 h_{fg} latent heat of vaporization [J/kg]
 k thermal conductivity [W/m-°C]

k_m effective thermal conductivity [W/m-°C]
 K permeability of the porous medium [m²]
 L_e length of the evaporator [m]
 L_a length of the adiabatic region [m]
 L_c length of the condenser [m]
 p pressure [Pa]
 $q(z)$ local rate of heat transfer per unit length [W/m]
 Q_{total} total amount of heat entering and leaving the heat pipe [W]
 R_0 radius of the heat pipe [m]
 Re_p pore Reynolds numbers, $Re_p =$
 r_c pore radius of the wick structure [m]
 r, z radial and axial coordinates
 S_ϕ source term in the generic property ϕ
 V_r, V_z reduced velocities in the r and z direction respectively [m/s]
 V_w reduced blowing and suction velocity at the condenser and evaporator respectively [m/s]

v_i	actual velocity in the "i" direction in the micro-channel of the porous medium [m/s]
\bar{v}_i	average velocity within the void space of the porous medium [m/s]
v'_i	local spatial deviation in the "i" direction within the void space [m/s]
\bar{V}_i	Darcy velocity in the "i" direction [m/s]
t	time [s]
t_w	thickness of the wick structure [m]
t_{wall}	thickness of the solid wall of the heat pipe [m]
T_∞	ambient temperature [°C]

Greek Letters

ε	porosity
ρ	density [kg/m ³]
σ	surface tension [N/m]
ϕ	generic property
μ	dynamic viscosity [kg/m-s]
Γ	diffusivity for the generic property ϕ

Subscripts

s	solid wall
l	liquid
v	vapor

REFERENCES

- [1] Bear, J., *Dynamics of Fluids in Porous Media*, Dover Publications, Inc., New York (1988)
- [2] Cao, Y. and Faghri, A., Transient two-dimensional compressible analysis for high temperature heat pipes with pulsed heat input, *Numerical Heat Transfer, Part A*, vol. 18, pp. 483-502 (1990).
- [3] Chi, S.H., *Heat Pipe Theory and Practice*, McGraw-Hill, New York (1976).
- [4] El-Genk, M. S. and Huang L., An experimental investigation of the transient response of a water heat pipe, *International Journal of Heat and Mass Transfer*, Volume 36, Issue 15, Pages 3823-3830 (1993).
- [5] Faghri, A., *Heat Pipe Science and Technology*, Taylor & Francis, Washington, D.C (1995).
- [6] Faghri, A., Frozen start-up behavior of low-temperature heat pipes, *International Journal of Heat and Mass Transfer*, Volume 35, Issue 7, pp.1681-1694 (1992).
- [7] Faghri, A. Gogineni, S. and Thomas, S., Vapor Flow Analysis of An Axially Rotating Heat Pipe, *Int. J. Heat Mass Transfer*, Vol. 36, pp. 2293-2303 (1993) .
- [8] Ferziger J.H. and Peric M., *Computational Methods for Fluid Dynamics*, Springer-Verlag, Berlin, Heidelberg (1996).
- [9] Gray, V., The Rotating Heat Pipe-A Wickless, Hollow Shaft for Transferring High Heat Fluxes, ASME-AIChE Heat Transfer Conference, Minneapolis, Minnesota (1969).
- [10] Gutierrez, G., (2002), *Investigation of Heat Pipes for Drilling Applications*, Ph.D. Dissertation, University Of Wisconsin-Milwaukee.
- [11] Harley, C. and Faghri, A., Two-Dimensional Rotating Heat Pipe Analysis, *ASME J. Heat Transfer*, Vol. 117, No. 1, pp. 202-208 (1995).
- [12] Issacci, F., Catton, I. And Ghoniem, N.M., Vapor Dynamics of heat pipe start-up, *ASME J. Heat Transfer*, Vol. 113, pp. 985-994 (1991).
- [13] Jen, T.C., Gutierrez, G., Eapen S., Barber, G., Zhao, H., Szuba, S., Manjunathaiah, J., and Labataille, J., Investigation of Heat Pipes Cooling in Drilling Applications Part I: Preliminary Numerical Analysis and Verifications, *International Journal of Machine Tool and Manufacture*, Volume 42, Issue 5, pp. 643-652 (2002).
- [14] Khosla, P.K. and Rubin, S.G., A Diagonally Second Order Accurate Implicit Scheme, *Computers Fluids*, 2, 207-209 (1974).
- [15] Patankar, S.V., *Numerical Heat Transfer and Fluid Flow*, Hemisphere Publishing Corp., Washington, D.C (1980).
- [16] Peterson, G.P., *An Introduction to Heat Pipes: Modeling, Testing, and Applications*, Wiley, New York (1994).
- [17] Sobhan, C.B., Garimella, S.V. and Unnikrishnan, V.V., A Computational Model for the Transient Analysis of Flat Heat Pipes, ASME paper, International Heat Transfer Conference, Orlando, FL (2000).
- [18] Tournier, J. M. and El-Genk M. S., A heat pipe transient analysis model, *International Journal of Heat and Mass Transfer*, Volume 37, Issue 5, Pages 753-762 (1994).
- [19] Tournier, J. M. and El-Genk M. S., A vapor flow model for analysis of liquid-metal heat pipe startup from a frozen state, *International Journal of Heat and Mass Transfer*, Volume 39, Issue 18, pp. 3767-3780 (1996).
- [20] Van der Vost, H.A., BI-CGSTAB: A Fast and Smoothly Converging Variant of BI-CG for the Solution of Non-Symmetric Linear Systems, *SIAM J. Sci. Stat. Comput.*, 13, 631-644 (1992).
- [21] Van Doormal, J.P. and Raithby, G.D., Enhancements of the SIMPLE Method for Predicting Incompressible Fluid Flows, *Numerical Heat Transfer*, 7, 147-163 (1984).